

## Impurity Concentrations in the RI-mode in TEXTOR-94

R. Jaspers<sup>1</sup> and H.L.M. Widdershoven<sup>1,2</sup>

<sup>1</sup>*FOM-Instituut voor Plasmafysica 'Rijnhuizen', Association EURATOM-FOM, P.O.Box 1207, 3430 BE Nieuwegein, The Netherlands\**

<sup>2</sup>*Institut für Plasmaphysik, Forschungszentrum Jülich GmbH, EURATOM association D-52425 Jülich, Germany\**

### 1. Introduction

An enhanced confinement regime, the Radiative Improved (RI)-mode, is obtained in TEXTOR-94 during high density, additionally heated discharges with a radiating mantle. This mode follows the same scaling as the Linear Ohmic Confinement regime and is thus identified as one of the most fundamental tokamak operational regimes [1]. It combines simultaneously many attractive features for a reactor, such as high density, good energy confinement, steady state operation and power exhaust by edge cooling [2]. The main concern will be the compatibility of the impurity seeding with the required low central  $Z_{\text{eff}}$  value.

A radiative mantle can be obtained in TEXTOR-94 by neon or argon seeding. With freshly siliconised wall coating even no extrinsic impurity is necessary. In the present paper the impurity concentrations of the main elements in all these RI-mode cases at TEXTOR-94 are measured with the Charge eXchange Recombination Spectroscopy (CXRS). The same diagnostic is used to determine  $Z_{\text{eff}}$  profiles from bremsstrahlung.

The impurity content has, apart from diluting the plasma and creating the radiative mantle, a beneficial effect on the confinement since a relation between the impurity content and the trigger of the transition to the RI-mode is found [3].

### 2. $Z_{\text{eff}}$ scaling in RI-mode plasmas

For radiative plasmas a semi-empirical scaling law of  $Z_{\text{eff}}$  has been derived by several authors [4,5]:

$$Z_{\text{eff}} = 1 + \alpha P_{\text{rad}} / (S \bar{n}_e^2), \quad (1)$$

where  $\alpha \approx 7$ ,  $P_{\text{rad}}$  the radiated power (in MW),  $S$  the radiating surface (in m<sup>2</sup>) and  $\bar{n}_e$  the line averaged electron density (in 10<sup>20</sup> m<sup>-3</sup>). To check the validity of this scaling for RI-mode conditions in TEXTOR-94,  $Z_{\text{eff}}$  is plotted versus  $P_{\text{rad}}$  in Fig. 1a. The data were taken in discharges where neon is injected to reach the high confinement. All discharges have the same line averaged electron density  $\bar{n}_e = 5.10^{19} \text{ m}^{-3}$ , total input power  $P_{\text{tot}} = 4.0$  MW, Plasma current  $I_p = 400$  kA and magnetic field  $B_t = 2.25$  T. Close agreement with Eq. (1) is found. In Fig. 1a the neon and carbon concentrations measured with the CXRS diagnostic are also included.

The neon concentration rises linearly with  $P_{\text{rad}}$  whereas carbon shows a slight decrease as a result of the lower edge temperatures. Note that to obtain correct carbon and neon concentrations from the CXRS measurements, the effect of excited beam particles had to be taken into account [6,7]. These particles contributed up to 75% of the total CXRS signal for the beam energies used in these experiments ( $E_{\text{beam}} = 20\text{-}25$  keV/amu).

---

\* Partner in the Trilateral Euregio Cluster

The  $Z_{\text{eff}}$ -values are taken from bremsstrahlung measurements of a tangential line of sight through the plasma center. Although this is in fact a line integrated measurement, the result will be close to the central value due to the relatively long pathlength through the center and the  $n_e^2$  dependence of bremsstrahlung. The  $Z_{\text{eff}}$  as deduced from CXRS measurements were well within the uncertainties of the bremsstrahlung results. These, nevertheless, have large uncertainties ( $>15\%$ ) especially due to the effect of excited beam particles.

In Fig.1b. the  $n_e$  dependence of  $Z_{\text{eff}}$  is investigated for a series of discharges having the same  $P_{\text{tot}}=2.6$  MW,  $P_{\text{rad}}=2.0$  MW and  $I_p=400$  kA. As expected from Eq. 1 a  $n_e^{-2}$  dependence is found. Furthermore, this figure shows that  $Z_{\text{eff}}$  is nearly independent of the radiating impurity used. No different scaling becomes apparent whether neon, silicon or argon is used as radiator. Finally, in Fig. 1c the same datapoints are plotted against Eq.1 to demonstrate the quantitative agreement with this equation, where  $\alpha=7$  has been inserted.

The observations that a)  $Z_{\text{eff}}$  is inversely proportional to  $n_e^2$ , b) the energy confinement in the RI-mode scales linearly with  $n_e$  [1] and c) operation of the RI-mode at densities in excess of the empirical Greenwald limit is possible, shows that the impurity content might be tolerable under high confinement conditions with high radiated power fractions at high densities.

### 3. Profile effects

As shown in the previous section the impurity content in RI-mode discharges is globally described by Eq. (1). The question whether the averaged value of  $Z_{\text{eff}}$  is a good representation of the impurity content is not yet addressed. Accumulation of high  $Z$ -elements might occur in special discharge conditions [8], and the peaking of the neon profiles in the plasma centre when sawteeth disappear has been reported from ASDEX-U [9]. However, in the TEXTOR-94 RI-mode no accumulation has been observed even in non-sawtoothed phases of the discharge. Moreover, there are indications that the  $Z_{\text{eff}}$  profiles are even hollow, as shown in Fig. 2a.

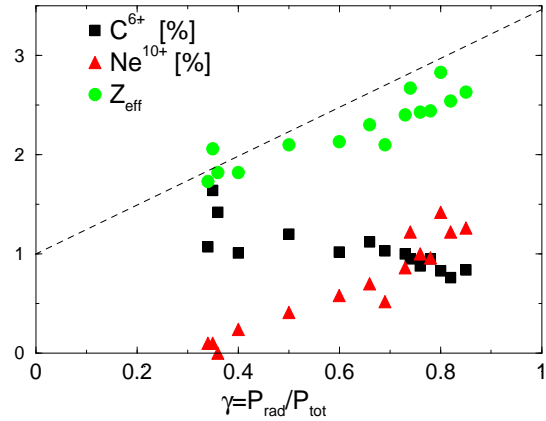


Fig 1a:  $Z_{\text{eff}}$ , carbon concentration and neon concentration as deduced from CXRS for RI-mode discharges as a function of radiated power fraction  $\gamma$ . The curve according to Eq. 1 is shown by the dotted line.

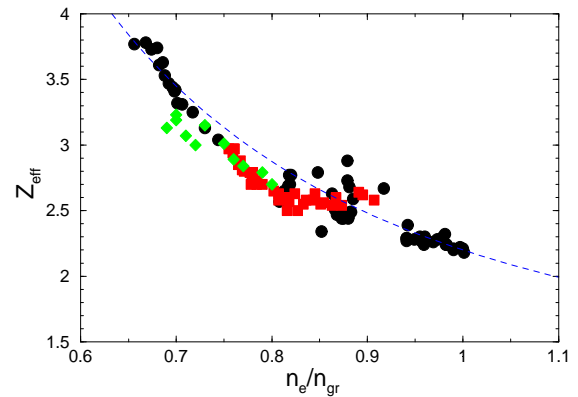


Fig.1b:  $Z_{\text{eff}}$  as a function of density for RI-mode discharge with different radiators: circles for neon, squares for silicon and diamonds for argon. The curve from Eq. 1 is shown by the dashed line.

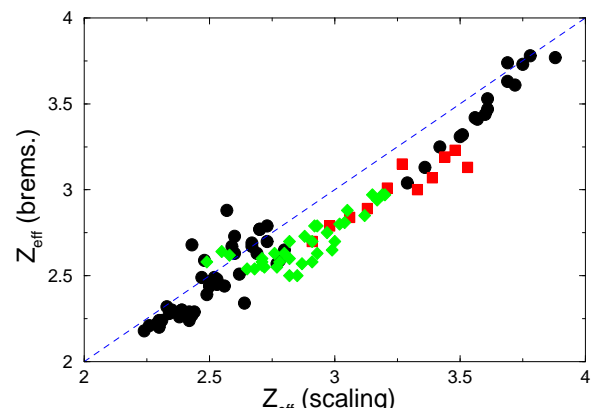


Fig 1c: For the same data as in Fig 1b, the measured  $Z_{\text{eff}}$  is plotted against the  $Z_{\text{eff}}$  scaling.

A similar feature is found in modelling the profiles with the predictive transport code RITM [3] or by comparing with flux measurements at the edge [10]. The profiles of the main impurities  $C^{6+}$  and  $Ne^{10+}$  are presented in Fig.2b. Although a considerable uncertainty in the centre will be due to the substantial beam attenuation, even here a slight hollowness of the profiles can be recognized. This will be even more pronounced when the lower ionization stages are added to the impurity profiles. The relatively low dilution in the centre is corroborated by the neutron measurements [11].

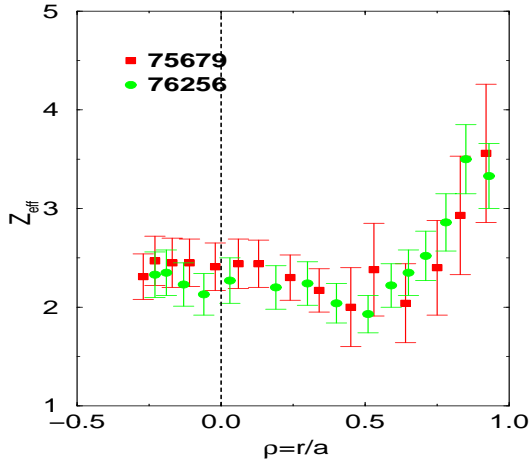


Fig.2a:  $Z_{eff}$  profiles as determined from Abel inversion of tangential bremsstrahlung measurements for two RI-mode discharges with neon as seeded impurity; one with boronized (75679) and one with siliconized wall conditions (76256). No clear difference is observed. In both cases a slightly hollow profile is observed.

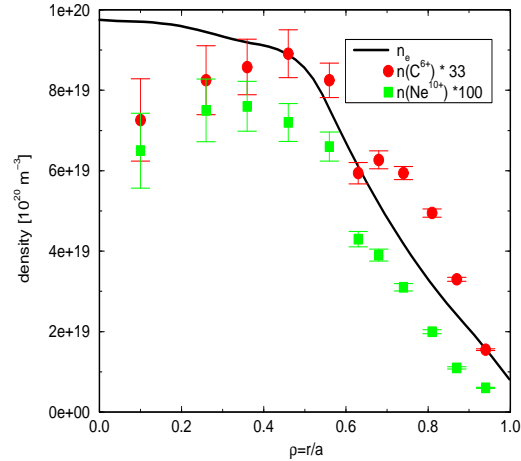


Fig. 2b: Profiles of the main impurities carbon and neon in a typical RI-mode discharge, compared with the electron density. Note the slight hollowness of the impurity profiles, which is even more pronounced when the not fully stripped ions in the outer regions are added.

#### 4. Effect of impurities in the confinement transition

In the present model to explain the confinement transition from the normal L-mode to the RI-mode, the impurities play a crucial role [3]. The proposed mechanism is based on the suppression of the toroidal ion temperature gradient (ITG) instability by the seeding of the impurities, succeeded by the peaking of the electron density profile. Following this, the confinement is improved and the transport is dominated by the dissipative trapped electron (DTE) instabilities. In that case a linear increase of confinement with density is predicted in agreement with observations.

More specifically in the model of Ref. [3] a transition to the RI-mode will occur when the ITG turbulence is suppressed which occurs for an mean ion charge  $\langle Z \rangle$  given by:

$$\langle Z \rangle = \frac{4(1-0.67p)}{\varepsilon_i p^2}; \quad \text{with} \quad p = \frac{d \ln n}{d \ln T_i}; \quad \varepsilon_i = -\frac{R}{2} \frac{d \ln T_i}{dr} \quad (2)$$

For a transition from the L (where the peaking  $p$  is small,  $p \approx 0.37$ ,  $\varepsilon_i \approx 9$ , at half radius) to the RI-mode, and relating this  $\langle Z \rangle$  to  $Z_{eff}$ ,  $Z_{eff} = 2.4$  is predicted for the discharge displayed in Fig.3. For a back transition from RI-mode to L-mode confinement a lower value of  $\langle Z \rangle$  is requested, since the peaking factor in the RI-mode is higher.

One discharge is shown in Fig.3 which contains both an L-RI transition and an RI-L back transition. The L-RI transition is triggered by the injection of neon, increasing the radiated power and  $Z_{\text{eff}}$  to a value above  $\langle Z \rangle$  as calculated from Eq.(2).

Since it was shown in the preceding sections that a decrease of  $P_{\text{rad}}$  or an increase of  $n_e$  reduces  $Z_{\text{eff}}$ , one could expect a back transition when  $Z_{\text{eff}}$  reduces too much. In Fig. 3 the back transition is indeed governed by the decrease in  $P_{\text{rad}}$  and a simultaneous increase in  $n_e$ . At a certain value a roll over to lower confinement occurs (which is not due to MHD activity). Moreover, the back transition occurs at a lower  $Z_{\text{eff}}$ . Apart from that, the close relation with Eq. (1) is shown as well.

Although this definitively is no conclusive confirmation of the model of Ref. [3], it nevertheless shows that for the investigated L-RI transitions,  $Z_{\text{eff}}$  is increasing, whereas for the RI-L changeover a decline in impurity concentration is observed.

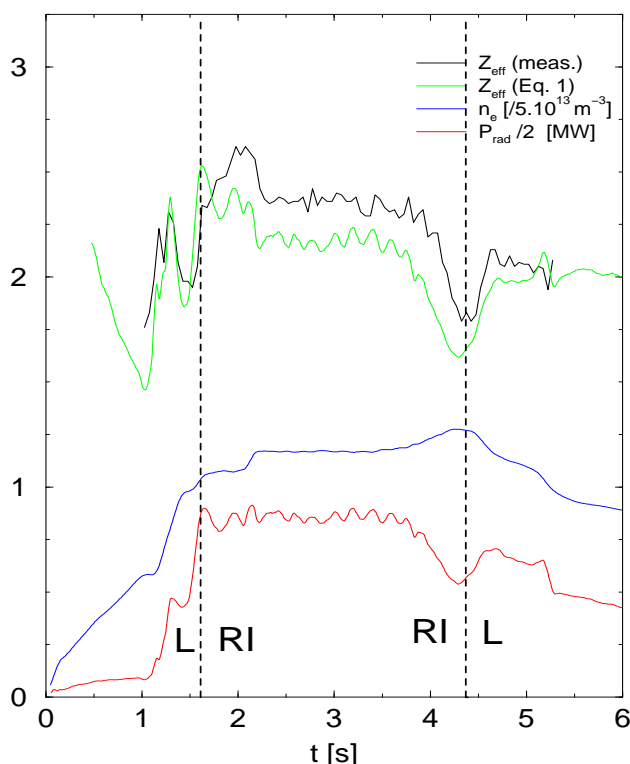


Fig. 3: Time traces for an RI-mode discharge of  $n_e$ ,  $P_{\text{rad}}$ ,  $Z_{\text{eff}}$  as measured and predicted from Eq. 1. The transitions from L to RI-mode and back are indicated.

## 5. Summary

The impurity content in the RI-mode as expressed by  $(Z_{\text{eff}}-1)$  scales  $P_{\text{rad}}/n_e^2$ . No difference concerning  $Z_{\text{eff}}$  was observed whether neon, argon or silicon was utilised as radiator. There are indications that the profile of  $Z_{\text{eff}}$  or the impurities Ne or C are higher in the edge or radiating zone than in the centre.

The confinement improvement of the RI-mode is thought to be triggered by the increased impurity content. This suppresses the ITG turbulence, resulting in a peaked density profile and reduced transport. Observations show indeed that The time evolutions of  $Z_{\text{eff}}$  in an L-RI is accompanied by a rise in  $Z_{\text{eff}}$  and an RI-L transition with a decrease in  $Z_{\text{eff}}$ .

## references

1. R.R. Weynants et al., Proc. 17<sup>th</sup> IAEA Conf. on Plasma Phys. and Control. Fusion, Yokohama (1998).
2. A.M. Messiaen et al., Phys. Rev. Lett. 77 (1996) 2487.
3. M.Z. Tokar' et al, Confinement mechanisms in the radiatively improved mode, this conference.
4. K. Behringer et al., Proc. 11<sup>th</sup> IAEA Conf. on Plasma Phys. and Control. Fusion, Kyoto (1986) 197.
5. G. Matthews, Proc. 4<sup>th</sup> European Fusion Workshop, Stockholm (1996).
6. D. G. Whyte et al., Nucl. Fusion 38 (1998) 387.
7. R. Jaspers et al., 24<sup>th</sup>EPS Conf. Contr. Fusion and Plasma Phys., Berchtesgaden, 21A (1997) IV-1713
8. J. Rapp et al., Plasma Phys. Control. Fusion 39 (1997) 1615.
9. R. Dux et al., Plasma Phys. Control. Fusion 38 (1996) 989.
10. B. Unterberg et al., Plasma Phys. Control. Fusion 39 (1997) B189.
11. G. van Wassenhove, 24<sup>th</sup>EPS Conf. Contr. Fusion and Plasma Phys., Berchtesgaden, 21A (1997) IV-1679.